NACA TN 3833
TN
3833
c. 1
TECH LIBRARY KAFB, NM
0066755

NATIONAL ADVISORY COMMITTEE FOR AERONAUTICS

TECHNICAL NOTE 3833

STABILITY LIMITS AND BURNING VELOCITIES OF LAMINAR HYDROGEN-AIR FLAMES AT REDUCED PRESSURE

By Burton Fine

Lewis Flight Propulsion Laboratory
Cleveland, Ohio

Washington
November 1956

AFMDC

TECH LIBRARY KAFB, NM
0066755

NATIONAL ADVISORY COMMITTEE FOR AERONAUTICS

TECHNICAL NOTE 3833

STABILITY LIMITS AND BURNING VELOCITIES OF LAMINAR HYDROGEN-AIR FLAMES AT REDUCED PRESSURE

By Burton Fine

SUMMARY

Laminar burning velocity was measured at pressures of 1 atmosphere and below and critical boundary velocity gradient for flashback at pressures below 1 atmosphere over a range of compositions for hydrogen-air burner flames. Pressure exponents of 0.23 for burning velocity and 1.35 for flashback velocity gradient were found. In both cases the pressure dependence was independent of composition between equivalence ratios of about 1 and 2. A more general correlation relating flashback velocity gradient, burning velocity, and quenching distance conformed to the simple quenching model of Lewis and von Elbe. From this correlation and recent thermal equations for flame propagation, a global reaction order of 2.2 to 2.3 was calculated.

A complete laminar stability loop was obtained for one particular burner diameter and equivalence ratio. Its shape is discussed in terms of quenching regions, normal laminar regions, and possible regions of laminar-turbulent transition.

INTRODUCTION

In the past, various relations have been reported among measured properties of burner flames. In some cases, it has been possible to relate these empirical correlations to theories of flame propagation and thus obtain an insight into the mechanism of combustion. This report describes a study of certain of these relations for hydrogen-air burner flames over a range of pressures and compositions.

Two combustion parameters, laminar burning velocity and critical laminar boundary velocity gradient for flashback, were measured as functions of composition and pressure. Treatment of data was based on an examination of the relation (symbols defined in the section SYMBOLS)

$$g_f = U_b/\delta \tag{1}$$

which was first proposed as a definition of the penetration distance or "dead space" between a burner flame and a cold wall (ref. 1, p. 286). It has generally been assumed that this penetration distance is proportional to the quenching distance:

$$\delta = (1/C)d_q \tag{2}$$

and that the value of C depends mainly on the channel geometry. Thus, g_f is assumed proportional to U_b/d_q. On the basis of thermal theories of flame propagation, it has been proposed that this quotient, and hence g_f, is a function only of a reaction rate within the flame zone. It has been suggested (ref. 2, p. 5) that g_f might serve as a direct measure of reaction rate. Therefore, it was of interest to examine to what extent the relation

$$g_f = CU_b/d_q \tag{3}$$

would hold for the hydrogen-air system. This correlation was studied in detail, since the quenching distance for hydrogen and air had been previously measured over a range of pressures and compositions (ref. 3).

Laminar burning velocity was measured at pressures of 1 atmosphere and below and critical boundary velocity gradient for flashback at pressures below 1 atmosphere over a range of compositions. The flames studied were stabilized above long burner tubes whose diameters ranged from 0.331 centimeter to 1.459 centimeters. In addition, sufficient data on blowoff at reduced pressures were obtained to give a general idea of the size and shape of the complete laminar stability loop.

SYMBOLS

The following symbols are used in this report:

A area of flame front, cm^2

b measured base of flame, cm

C coefficient relating penetration distance to quenching distance

d burner diameter, cm

d_q quenching distance, cm

E activation energy, kcal/mole

g critical boundary velocity gradient, sec^{-1}

h height measured on flame front, cm

l distance across flame front, cm

M magnification factor

m reaction order

n pressure exponent

P ambient pressure, cm Hg

R gas constant, cal/(mole)(^{o}K)

r,r' coefficients which account for temperature dependence of transport properties in active flame and quenched flame, respectively

T absolute temperature, ^{o}K

U average velocity, cm/sec

V volume flow rate, cm^3/sec

δ penetration distance, cm

Φ equivalence ratio, fuel-air ratio divided by fuel-air ratio for stoichiometric mixture

Subscripts:

b burning

f flashback

l linear

n normal flame conditions

q quenching, quenched-flame conditions

u burning velocity

0 initial conditions

Superscript:

o determined at reference conditions of critical-flow orifice calibration (about 1 atm pressure)

CI-1 back

APPARATUS

A sketch of the combustion system is shown in figure 1. The combustion chamber was cylindrical and water jacketed around its lateral surface. It had an outside diameter of 12 inches and a height of 24 inches. Two opposing rectangular windows $3\frac{1}{2}$ inches by 12 inches were cut in the sides and fitted with glass windows, which were held in place by screws and rubber gaskets. The combustion chamber led through a connecting arm fitted with baffles into a plenum chamber. The plenum was connected to a vacuum pump, which served as a general exhaust. The pressure within the system could be adjusted by a manual air bleed and was read from a manometer connected to a pressure tap. Cooling water was exhausted into the plenum in the form of a spray or curtain. This water curtain was designed to cool exhaust gases and prevent combustion arising in the combustion chamber from propagating into the plenum. The plenum itself could be periodically drained.

The burner had a length of about 50 inches and a nominal diameter of 3/4 inch. It was fitted with tubular inserts about 5/8, 3/8, 1/4, and 1/8 inch in diameter and was water jacketed. The burner was fitted into a round opening in the bottom of the combustion chamber by a pressure seal.

Incoming fuel and air were metered separately through calibrated critical flow orifices and then mixed and ignited at the burner port by a retractable spark igniter. This ignition source was effective down to pressures of about 0.1 atmosphere. Sintered bronze flame arresters (ref. 4) were used to prevent flashed-back flames (or flames which had flashed back) from propagating upstream. Fuel flow was monitored by a manually set differential thermal switch which was activated by a thermocouple placed above the flame. If the temperature of the thermocouple fell below a set value, because of loss of flame, fuel was automatically cut off and the system was purged with nitrogen. These devices were installed to prevent accumulation of unburned fuel in the combustion and plenum chambers. For purposes of ignition, the differential thermal switch contained a manual override.

Tank hydrogen (98 to 99 percent H_2) and tank compressed air (water pumped) were used without further purification.

PROCEDURE

Stability Limit Measurement

The procedure used for determining blowoff and flashback limits was essentially that reported in reference 5. A stable flame was

established; then the pressure was slowly varied, at constant mass flow, until the flame was lost. This procedure was carried out at constant initial reactant temperature.

The average stream velocity at which flame loss occurred was obtained as a function of the ambient pressure, the burner diameter, and the nominal volume flow rate for 1 atmosphere pressure by the expression

$$U_f = \frac{4V^o}{\pi d^2} \frac{P^o}{P} \tag{4}$$

The quantity V^o was obtained from the calibration curve of the critical-flow orifices used. The reference temperature and pressure for calibration were chosen so that day-to-day fluctuations in temperature and barometric pressure caused negligible fluctuations in V^o. For ambient pressures of less than 20 centimeters of mercury, the barometric pressure was corrected to 0° C. At higher pressures, this correction was insignificant.

Flames were sufficiently luminous to be visible in a darkened room, although they appeared extremely faint below 0.2 atmosphere. In most cases, blowoff could be detected visually with reasonable sharpness. In the case of particularly faint flames, blowoff could be detected because the thermocouple of figure 1 ceased to glow rather suddenly after the flame was lost. Thus, blowoff was measured down to 0.05 atmosphere.

It was observed that flashback was sharp and vigorous at higher pressures but became less well defined at lower pressures. In these regions intermediate stages of "tilted" flames were observed as the pressure was slowly increased. Observations of this sort are reported in reference 6. Because of the existence of a narrow pressure range yielding tilted or partially flashed-back flames, it was necessary to establish a criterion for the pressure at which a flame flashed back. This was taken to be that pressure at which a stable flame could not be maintained above the burner port. By this criterion, partially flashed-back flames were considered as completely flashed back. The pressure range of partial flashback was extremely narrow, and an uncertainty of only a few millimeters of mercury was introduced by this procedure.

Measurements were made with burners having diameters of 1.459, 1.016, and 0.546 centimeter.

Burning Velocity Measurement

Schlieren photographs were taken of laminar Bunsen flames at about unit magnification. A high-pressure mercury arc was used to give an exposure of about 5 microseconds.

The operating procedure was as follows: By manual adjustment of the pumping rate and the rate of air intake through the bleed, the pressure within the combustion chamber was set at a desired constant value. The pressure was known to about ±0.2 centimeter of mercury. Flames were established above the burner port and photographed; composition was varied while pressure was held constant and total mass-flow rate was changed only slightly. Measurements were made at pressure levels of 74, 46, 29, and 16 centimeters of mercury. Corresponding burner diameters were 0.331, 0.546, 1.016, and 1.459 centimeters. Thus, burner size was, roughly, inversely proportional to the pressure (ref. 5). Corresponding Reynolds numbers were about 1400, 2100, 1200, and 850 and were, in all cases, an order of magnitude greater than the Reynolds number for a nearly quenched flame. In this way, cooling of the flame by the tube wall was avoided (ref. 7). In addition, conditions were adjusted so that the flames studied were far removed from the blowoff limit; thus there was no appearance of lifted flames at low pressures. A few measurements were made at 1 atmosphere with a 0.546-centimeter burner. Results were not significantly different from those obtained with a 0.331-centimeter burner. An over-all composition range of 27 to 64 percent hydrogen was covered, but the total spread was not obtained at all pressures.

4178

Burning velocity was obtained by the relation

$$U_b = \frac{V^o}{A}\frac{P^o}{P} \tag{5}$$

The total area was calculated from measurements on the photographs by the approximation

$$A = \frac{\pi}{2}\left[(b + l)\sqrt{h_1^2 + \left(\frac{b - l}{2}\right)^2} + l\sqrt{h_2^2 + \frac{l^2}{4}}\right]\frac{1}{M^2} \tag{6}$$

The symbols used in equation (6) may be clarified by referring to the following sketch:

4178

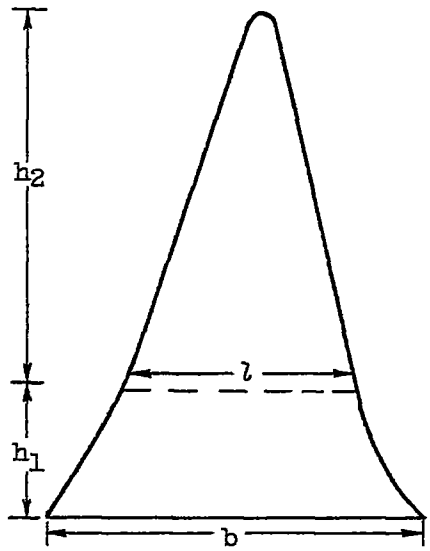

The approximation attempts to correct for the departure of the flame from the shape of a cone in a simple fashion. The relative magnitudes of h_1 and h_2 were chosen according to the size and shape of the flame. In many cases the curvature of the flame side was small enough that the simple approximation of a perfect cone gave results within 5 percent of these obtained by equation (6). In no case was the difference greater than 12 percent.

RESULTS AND DISCUSSION

Table I shows the critical flashback velocity and boundary velocity gradient as a function of ambient pressure, burner diameter, and equivalence ratio. Roughly, for a single equivalence ratio, the data for flashback velocity yield a family of parallel lines, one for each burner. An example is shown in figure 2. However, a more satisfactory correlation is obtained if the critical boundary velocity gradient is plotted against pressure. For fully developed Poiseuille flow, this is defined by the relation

$$g_f = 8U_l/d \tag{7}$$

As shown in figure 3, the correlation of g_f with ambient pressure is independent of burner diamter over an intermediate range of flow conditions. The correlation is best between $\Phi = 1.30$ and $\Phi = 1.80$ and is less satisfactory at the extremes of composition. Above a Reynolds number of about 1500, it fails completely. The pressure for flashback remains constant with increasing critical boundary velocity gradient and becomes a function of burner diameter.

The data shown in figures 2 and 3 are not exhaustive. However, they are sufficiently complete to permit a general discussion of the flashback portion of the stability curve. From consideration of the present data and the results given in reference 5 with acetylene flames, it may be inferred that the curve for laminar flashback has the following general shape:

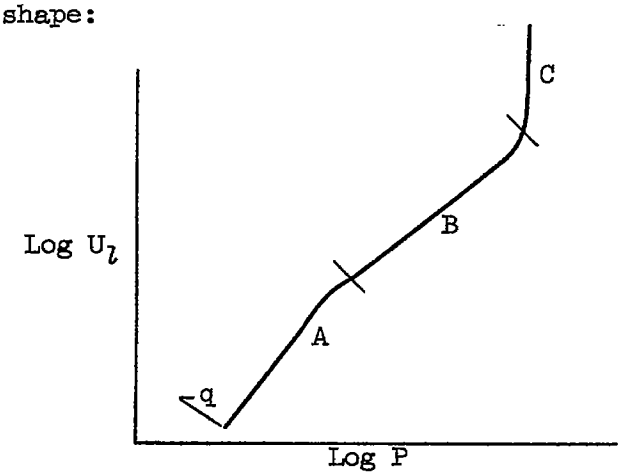

and may be divided into three parts as shown. The shape of this curve may be interpreted by referring to equation (1). In the B portion the burning velocity is assumed to have its normal value at a distance δ from the wall. In general, burning velocity and penetration distance will vary with pressure, and this will lead to a variation of g_f with pressure. As pressure is reduced, however, the reaction rate, which varies with P^2, decreases sharply while the rate of heat conduction to the wall remains about the same. Thus, at some low pressure, the volumetric heat-release rate becomes insufficient to maintain normal flame temperature; and the burning velocity is accordingly reduced. By equation (1), then, the flame will flash back at a lower boundary velocity gradient than would be expected from the normal effect of pressure on burning velocity. This is what is observed in region A. Finally, a pressure is reached below which the flame is cooled sufficiently to be fully quenched. This happens at point q.

One further point may be made with regard to flashback at low pressures. It has been assumed that the boundary velocity gradient, that is, the velocity gradient at the wall, is a good approximation for the actual flashback velocity gradient given in equations (1) and (3). However, this holds true only if the burner diameter is much larger than the penetration distance (or, accordingly, the quenching diameter). Thus, at sufficiently low pressures the actual flashback velocity gradient will become smaller than the boundary velocity gradient defined by equation (7). If, in figure 3, the actual velocity gradient were plotted instead of the boundary velocity gradient, the trend observed in the low-pressure region would be even more pronounced.

4178

The existence of region C cannot be explained in any detail. In this region the pressure at which the flame disappeared down the tube appeared independent of stream velocity for a particular burner but increased with decreasing burner diameter (fig. 2). That the Reynolds number associated with the beginning of each constant pressure region had a value of about 1500 suggests that laminar-turbulent transition is somehow involved. However, below Reynolds numbers of about 2200, the flames themselves appeared laminar and showed no evidence of instability or turbulence.

Data shown in figure 3 which lie in region B, the region of normal laminar flashback, have been correlated by a relation of the form

$$g_f \propto P^{n_f} \tag{8}$$

Between $\Phi = 0.95$ and $\Phi = 2.25$ n_f takes on values between 1.27 and 1.42. The scatter with composition is random and, therefore, n_f may be taken equal to 1.35 ± 0.08. For $\Phi = 0.80$, on the other hand, n_f has a value of about 2. Once again, this effect cannot be explained quantitatively but may be related to the unusually high diffusivity of hydrogen which, lean of stoichiometric, might drastically affect the burning velocity near the wall. In general, lean hydrogen-air flames are known to exhibit peculiar behavior (ref. 8).

Present results are compared with the data of reference 6, which were obtained at 1 atmosphere; consistently lower critical boundary velocity gradients (fig. 3) are predicted in reference 6. However, because of the large uncertain region of partial flashback reported in reference 6, agreement is considered satisfactory. Furthermore, in reference 6 the curve is drawn through the minimum values of the critical boundary velocity gradient for a given composition. Thus, the criterion of reference 6 for flashback was not the same as the one adopted in the present study. Figure 4 shows cross plots of g_f against percent hydrogen at various pressures; in addition, the curve of reference 6 is shown. It appears that a maximum occurs at about 38 percent hydrogen ($\Phi = 1.5$), and its position is independent of pressure.

Blowoff and General Stability Loop

The interpretation of blowoff data is difficult because of the fact that conditions under which a flame will blow off depend on the nature of the gases circulating near the base of the flame. For flames burning in open air, the critical boundary velocity gradient increases continuously with increasing fuel concentration at constant pressure (ref. 9). For completely shielded flames, however, only inert gases or combustion

products may circulate at the base of the flame. In this case, if the experimental conditions are sufficiently far removed from the quenching region, the critical boundary velocity gradient for blowoff will pass through a maximum at about the same concentration as for flashback at constant pressure (ref. 10, p. 84). The dimensions of the present apparatus are such that neither behavior is observed uniquely, and the resulting data cannot be interpreted in detail.

It is of interest, however, to examine a complete stability loop which is based on both blowoff and flashback measurements. An example is shown in figure 5 for $\Phi = 1.50$ (38 percent hydrogen) and $d = 1.459$. The general shape is similar to those reported for acetylene flames (ref. 5).

The flashback portion has been discussed previously. The blowoff portion of the stability loop may likewise be considered in three sections α, β, and γ of figure 5. In the α portion, the blowoff velocity increases with increasing pressure and merges into the turbulent region at high mass-flow rates. In the β portion, the blowoff velocity is independent of pressure; and, in the γ region, blowoff velocity actually decreases with increasing pressure. If, in the γ region at least, blowoff velocity depends on flame speed and penetration distance as expressed in equation (1), that region may be interpreted as a quenching region. Blowoff is assumed to occur when the stream velocity near the wall exceeds the burning velocity at every point (ref. 1, p. 288). Hence, if there is sufficient heat loss to the wall to cause a lower burning velocity than normal, the flame will blow off at a higher pressure than it otherwise would. This explanation assumes that the nature of gases circulating near the flame base will not qualitatively affect the result.

It has been assumed (ref. 5) that the flashback and blowoff curves intersect at point q in figure 5. The pressure at q would correspond to the pressure at which a tube 1.459 centimeters in diameter would quench a flame at $\Phi = 1.50$. If the pressure at q is predicted from the quenching-distance correlation given in reference 3, a pressure of 6.2 centimeters is obtained, which is in fair agreement with the result obtained by estimating the pressure at which the flashback and blowoff curves intersect. In figure 5, this occurs at about 7.3 centimeters. To cause the flashback and blowoff curves to intersect implies that point q defines an extinction velocity below which a flame of given composition and burning over a given tube cannot exist under any circumstances. It is possible, however, that the two curves might approach each other at first steeply but then asymptotically, in which case point q would define, within very narrow limits, a pressure but would not define a velocity.

The solid diamond in figure 5 shows about where on the stability diagram burning velocities were measured with a 1.459-centimeter burner. The Reynolds number at that point was about 850. This is more than an order of magnitude greater than the Reynolds number at quenching. Since 850 was the lowest Reynolds number at which burning velocity was measured, it may be assumed that quenching effects were absent in all cases.

Burning Velocity

Burning velocities are plotted in figure 6. At 1 atmosphere, the maximum value is about 304 centimeters per second and occurs at about 45 percent hydrogen ($\Phi = 1.95$). This value may be compared with values obtained by other methods. In reference 11, a maximum value of 298 is reported at 40 percent hydrogen. Reference 12 gives 310 centimeters per second at 41 percent hydrogen. The agreement is probably satisfactory for the different methods being used. No shift of the maximum composition is observed with change of pressure.

Burning velocities are not shown for concentrations much leaner than stoichiometric. Data in this region would be unreliable for two reasons. First, since the burning velocity peaks far into the rich region, burning velocities in the lean region would be subject to great uncertainty for little uncertainty in flow rates. Second, lean hydrogen-air burner flames have been observed to exhibit structure in the flame front so that burning velocity measured in the usual way has little meaning (ref. 8).

The experimental data are cross-plotted in figure 7 as functions of pressure at constant composition. A correlation of the form

$$U_b \propto P^{n_u} \tag{9}$$

was found with n_u varying randomly between 0.208 and 0.256 between $\Phi = 1.10$ and $\Phi = 1.90$; its average value over that range of composition is about 0.23. This pressure dependence is larger than the value of 0.09 reported in reference 12.

Relations Among Various Combustion Properties

The pressure exponent for quenching n_q was found to be about -1.11 between $\Phi = 1$ and $\Phi = 2$ (ref. 3). A general test of the validity of equation (3), therefore, would be to examine the relation

$$n_f = n_u - n_q \tag{10}$$

CI-2 back

Since, from the present investigation, $n_f = 1.35$ and $n_u = 0.23$, equation (10) holds very well. If the value of $n_u = 0.09$ reported in reference 11 is used, equation (10) does not hold as well. On the other hand, the relation

$$U_b d_q P = \text{constant} \tag{11}$$

has been experimentally observed and theoretically predicted (ref. 3). According to equation (11), therefore, the relation

$$n_u + n_q + 1 = 0 \tag{12}$$

should hold. In this case, however, the value of n_u reported in reference 11 gives better agreement than the present value.

The coefficient C, which is defined by equation (2), was calculated; the calculation was based on present data and the quenching data of reference 3. The value of C will depend on the geometry of the burner used for measuring d_q. Thus, it is found that in the region of normal laminar flashback the relation

$$g_f = 2.6 \frac{U_b}{d_q} \tag{13}$$

holds, where d_q represents the quenching distance between plane parallel plates. By reference to equation (2), then, it is found that

$$d_q = 2.6\delta \tag{14}$$

is in good agreement with simple quenching theory (ref. 1).

Reaction Order from Pressure Exponents

On the basis of a thermal theory of flame propagation, the following equations have been derived (ref. 3):

$$n_u = \frac{m}{2} - 1 + \frac{1}{2} r' \frac{d \ln T_n}{d \ln P} + \frac{E}{2RT_b} \frac{d \ln T_n}{d \ln P} \tag{15}$$

$$n_q = -\frac{m}{2} + \frac{1}{2} r \frac{d \ln T_q}{d \ln P} - \frac{E}{2RT_q} \frac{d \ln T_q}{d \ln P} \tag{16}$$

in which the pressure dependence of flame temperature is taken into account. The following assumptions have been made:

(1) The initial mixture is stoichiometric.

(2) The activation energy $E = 23$ kilocalories per mole (ref. 3).

(3) $d \ln T_n / d \ln P = d \ln T_q / d \ln P = 0.017.$ (17)

4178

(4) The coefficients r and r', which account for the temperature dependence of transport properties in the active flame and the quenched flame, respectively, are equal.

(5) The quenching temperature $T_q = 0.8\ T_n + 0.2\ T_0$ (ref. 3). (18)

Then, provided equation (3) is valid, equations (15), (17), and (18) may be combined to yield the expression

$$n_f = m - 1 + \frac{E}{2R} \frac{d \ln T_n}{d \ln P}\left(\frac{1}{T_n} + \frac{1}{T_q}\right) \tag{19}$$

With the aid of equation (17), this may be solved for the reaction order m to give a value of 2.25 ± 0.09. This result is in good agreement with the value 2.17 obtained from quenching data (ref. 3).

In a similar way, a reaction order may be obtained from the pressure exponent of burning velocity by use of equation (15). The result is insensitive to the value chosen for r'. Thus, a value of r' between 0 and 2 will lead to a reaction order in the range 2.32 to 2.36.

SUMMARY OF RESULTS

Laminar burning velocities and stability limits were measured at pressures below 1 atmosphere and over a range of compositions for hydrogen-air burner flames.

Laminar burning velocity for hydrogen-air flames was a maximum with about 45 percent fuel (equivalence ratio $\Phi = 1.95$) over a pressure range from 0.2 to 1 atmosphere; at 1 atmosphere, the maximum value was about 304 centimeters per second. Over the given pressure range and Φ of about 1 to 2, the following correlation was found:

$$U_b \propto P^{0.23}$$

where U_b is the average burning velocity and P is the ambient pressure.

For that intermediate portion of the laminar flashback curve between the region of partial quenching and the region corresponding to a Reynolds number greater than 1500, the following correlation is observed:

$$g_f \propto P^{1.35}$$

where g_f is the critical boundary velocity gradient for flashback. This is valid between $\Phi = 0.95$ and $\Phi = 2.25$. A more general relation

$$g_f = 2.6 \frac{U_b}{d_q}$$

where d_q is the quenching distance measured between plane parallel plates, is observed over a range of pressures and compositions. The coefficient 2.6 is in reasonable agreement with a simple physical model for quenching.

A global reaction order in the range from 2.2 to 2.3 has been calculated from observed pressure exponents and thermal-type equations for flame propagation.

Lewis Flight Propulsion Laboratory
National Advisory Committee for Aeronautics
Cleveland, Ohio, August 13, 1956

REFERENCES

1. Lewis, Bernard, and von Elbe, Guenther: Combustion, Flames and Explosions of Gases. Academic Press, Inc., 1951.

2. Wohl, Kurt, Kapp, Numer M., and Gazley, Carl: The Stability of Open Flames. Third Symposium on Combustion and Flame and Explosion Phenomena, The Williams & Wilkins Co. (Baltimore), 1949, pp. 3-21.

3. Potter, A. E., and Berlad, A. L.: The Effect of Fuel Type and Pressure on Flame Quenching. Paper presented at Sixth Symposium (International) on Combustion, New Haven (Conn.), Aug. 19-24, 1956.

4. Egerton, A. C., Everett, A. J., and Moore, N. P. W.: Sintered Metals as Flame Traps. Fourth Symposium (International) on Combustion, The Williams & Wilkins Co. (Baltimore), 1953, pp. 689-695.

5. Wolfhard, H. G.: Die Eigenschaften stationareer Flammen im Unterdruck. Zs. f. Tech. Phys., Bd. 24, Nr. 9, 1943, pp. 206-211.

6. von Elbe, Guenther, and Mentser, Morris: Further Studies of the Structure and Stability of Burner Flames. Jour. Chem. Phys., vol. 13, no. 2, Feb. 1945, pp. 89-100.

7. Gaydon, A. G., and Wolfhard, H. G.: Flames - Their Structure, Radiation and Temperature. Chapman & Hall (London), 1953, p. 21.

4178

8. Garside, J. E., and Jackson, B.: The Formation and Some Properties of Polyhedral Burner Flames. Fourth Symposium (International) on Combustion, The Williams & Wilkins Co. (Baltimore), 1953, pp. 545-552.

9. Bollinger, Lowell M., and Williams, David T.: Experiments on Stability of Bunsen-Burner Flames for Turbulent Flow. NACA Rep. 913, 1948. (Supersedes NACA TN 1234.)

10. Wohl, Kurt: Quenching, Flash-Back, Blow-Off - Theory and Experiment. Fourth Symposium (International) on Combustion, The Williams & Wilkins Co. (Baltimore), 1953, pp. 68-89.

11. Manton, John, and Milliken, B. B.: Study of Pressure Dependence of Burning Velocity by the Spherical Vessel Method. Proc. Gas Dynamics Symposium (Aerothermochem.), Northwestern Univ., 1956, pp. 151-157.

12. Burwasser, Herman, and Pease, Robert N.: Burning Velocities of Hydrogen-Air Flames. Jour. Am. Chem. Soc., vol. 77, no. 22, Nov. 20, 1955, pp. 5806-5808.

TABLE I. - FLASHBACK DATA FOR HYDROGEN-AIR FLAMES

Equivalence ratio, ϕ	Burner diameter, d, cm	Ambient pressure, P, cm Hg	Average flashback velocity, U_f, cm/sec	Flashback critical boundary velocity gradient, g_f, sec^{-1}
0.80	0.546	59.6	377	5,530
		60.0	492	7,200
		63.0	652	9,580
		62.5	1188	[a]17,350
	1.016	28.3	168	1,300
		29.4	219	1,724
		33.3	242	1,906
		35.6	277	2,181
		38.8	359	2,827
		41.1	448	3,428
		45.6	474	3,727
		45.4	588	4,630
		42.5	761	[a]5,988
		44.5	858	[a]6,659
		47.7	908	[a]7,045
.95	.546	46.0	243	3,561
		51.3	298	4,379
		55.6	348	5,097
		63.9	495	7,253
		68.9	575	8,425
		63.5	801	11,731
		62.5	960	[a]14,044
	1.016	22.1	199	1,567
		25.4	220	1,732
		24.5	234	1,843
		25.8	264	2,079
		25.5	265	2,084
		31.5	281	2,214
		27.0	296	2,331
		30.1	302	2,378
		33.7	350	2,755
		31.7	361	2,842
		38.2	406	3,194
		38.7	510	4,012
		38.6	550	4,329
		42.3	600	4,730
		38.7	803	6,319
		39.7	927	[a]7,291
	1.459	18.9	229	1,256
		20.0	281	1,541
		23.0	372	2,040
		25.1	416	2,281
		28.7	444	2,435
		28.2	502	2,752
		28.5	542	2,972
		30.0	583	3,197
1.10	.546	42.0	281	4,106
		47.8	335	4,911
		47.0	340	4,982
		52.6	385	5,643
		49.6	415	6,081
		51.5	477	6,989
		63.7	504	7,380
		55.9	514	7,531
		62.4	516	7,560
		67.3	634	9,289
		64.6	650	9,524
		71.9	730	10,696
		63.5	1118	[a]16,369
	1.016	21.0	219	1,724
		22.8	250	1,968
		25.0	281	2,213
		29.5	303	2,385
		28.8	324	2,551
		28.6	354	2,787
		31.6	388	3,055

Equivalence ratio, ϕ	Burner diameter, d, cm	Ambient pressure, P, cm Hg	Average flashback velocity, U_f, cm/sec	Flashback critical boundary velocity gradient, g_f, sec^{-1}
1.10	1.016	30.6	390	3,071
		34.3	424	3,341
		36.4	499	3,929
		36.6	503	3,959
		37.6	547	4,308
		39.6	668	5,247
		37.8	858	[a]6,750
		38.4	1000	[a]7,871
	1.459	16.7	268	1,470
		18.7	320	1,755
		21.3	418	2,292
		24.0	490	2,687
		25.0	571	3,131
		28.9	639	3,503
		28.9	683	3,745
		27.9	806	4,420
1.30	.546	38.5	320	4,689
		43.0	390	5,714
		48.2	457	6,696
		51.9	519	7,604
		55.0	553	8,103
		59.2	594	8,703
		62.1	631	9,245
		65.7	666	9,758
		66.5	724	10,608
		68.6	738	10,828
	1.016	19.9	252	1,984
		21.6	285	2,244
		25.0	330	2,598
		24.2	353	2,780
		25.9	278	2,976
		26.1	380	3,000
		28.7	453	3,570
		31.5	510	4,016
		31.4	516	4,070
		33.0	586	4,630
		36.2	621	4,890
		38.2	710	5,580
		39.1	738	5,811
		37.4	946	[a]7,449
		36.2	974	7,680
	1.459	11.8	147	800
		13.0	182	1,000
		13.8	217	1,190
		16.0	299	1,646
		18.0	350	1,919
		20.0	393	2,155
		22.4	489	2,681
		24.5	507	2,780
		24.8	565	3,098
		25.8	603	3,306
		24.9	789	4,326
1.50	.546	31.4	279	4,088
		35.8	359	5,260
		34.9	367	5,377
		40.2	413	6,051
		39.9	415	6,081
		43.2	466	6,828
		46.6	507	7,429
		45.6	517	7,575
		47.5	573	8,396
		50.9	590	8,645

Equivalence ratio, ϕ	Burner diameter, d, cm	Ambient pressure, P, cm Hg	Average flashback velocity, U_f, cm/sec	Flashback critical boundary velocity gradient, g_f, sec^{-1}
1.50	0.546	55.0	618	9,055
		54.5	621	9,099
		57.5	670	9,817
		56.9	684	10,022
		60.9	719	10,535
		60.4	725	10,623
		65.3	740	10,842
		64.0	750	10,989
	1.016	20.4	285	2,244
		20.2	288	2,268
		21.1	322	2,535
		23.2	328	2,583
		22.2	354	2,787
		25.2	389	3,063
		26.2	410	3,226
		28.0	450	3,543
		30.7	501	3,945
		35.9	563	4,433
		40.4	627	4,937
		40.5	742	5,842
	1.459	39.6	892	7,024
		8.9	73	400
		9.3	87	478
		10.8	119	653
		10.0	131	723
		11.9	151	830
		12.0	165	908
		13.2	217	1,195
		16.4	312	1,711
		19.4	385	2,111
		21.8	454	2,489
		23.9	515	2,824
		25.4	578	3,169
		26.8	642	3,520
1.80	.546	39.1	384	5,330
		44.0	443	6,490
		49.1	503	7,365
		52.8	568	8,300
		56.1	623	9,100
	1.016	20.3	272	2,142
		22.6	309	2,433
		24.8	340	2,677
		28.1	397	3,126
		33.0	500	3,937
		37.2	593	4,669
		40.8	669	5,268
		42.3	728	5,732
	1.459	9.9	131	715
		12.0	165	908
		15.4	267	1,466
		17.4	314	1,725
		20.4	395	2,165
		23.4	459	2,520
		25.8	525	2,885
		27.1	554	3,038
		28.1	597	3,280
2.25	.546	46.7	352	5,150
		50.7	430	6,298
		57.0	468	6,850
		61.7	520	7,600
		67.7	557	8,150
	1.016	23.8	265	2,090
		26.2	295	2,330
		28.4	329	2,590
		34.6	365	2,830
		38.5	415	3,260
		42.3	453	3,570
		44.6	500	3,940

[a]Turbulent flames.

4178

CI-3

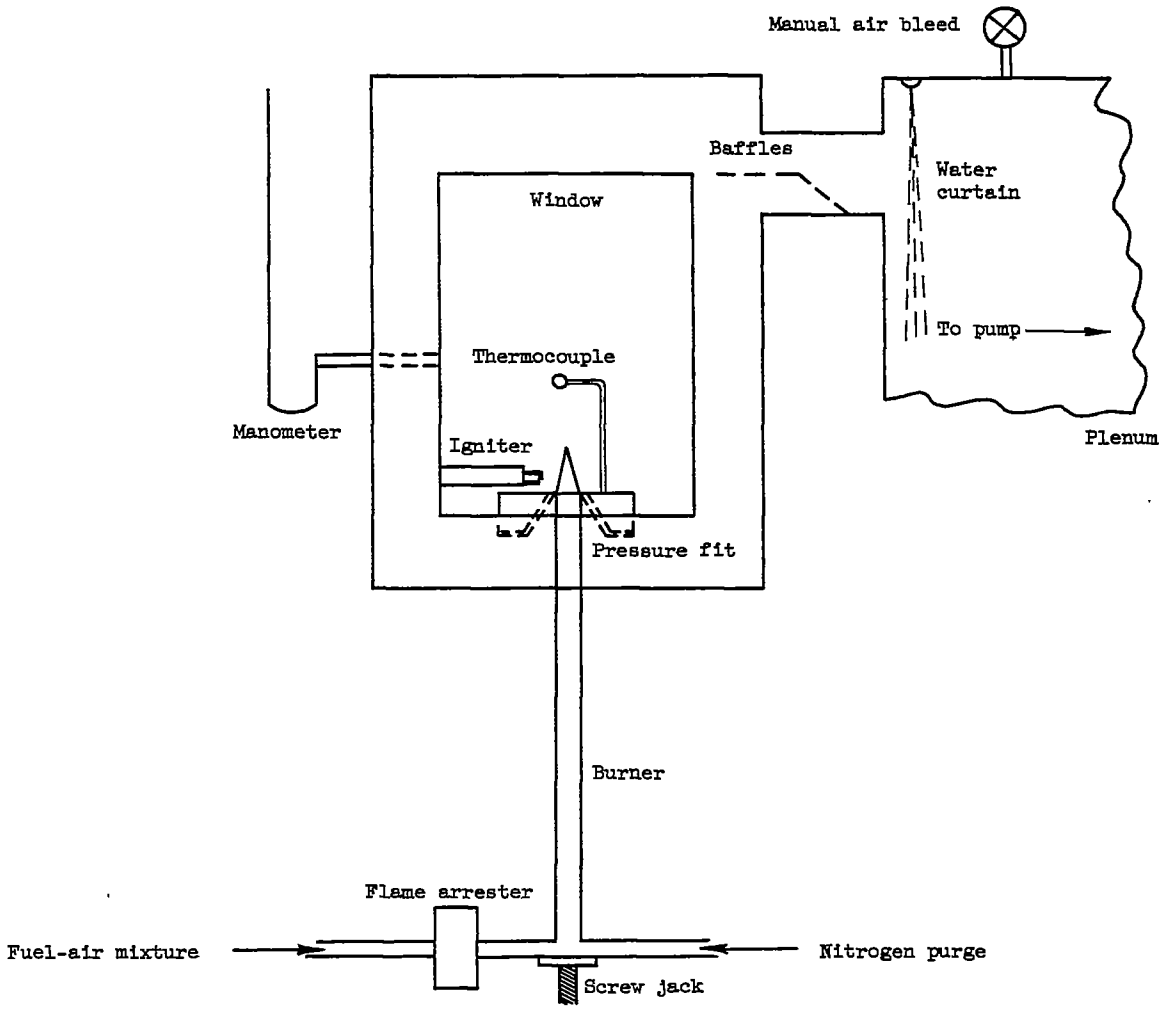

Figure 1. - Combustion chamber.

4178

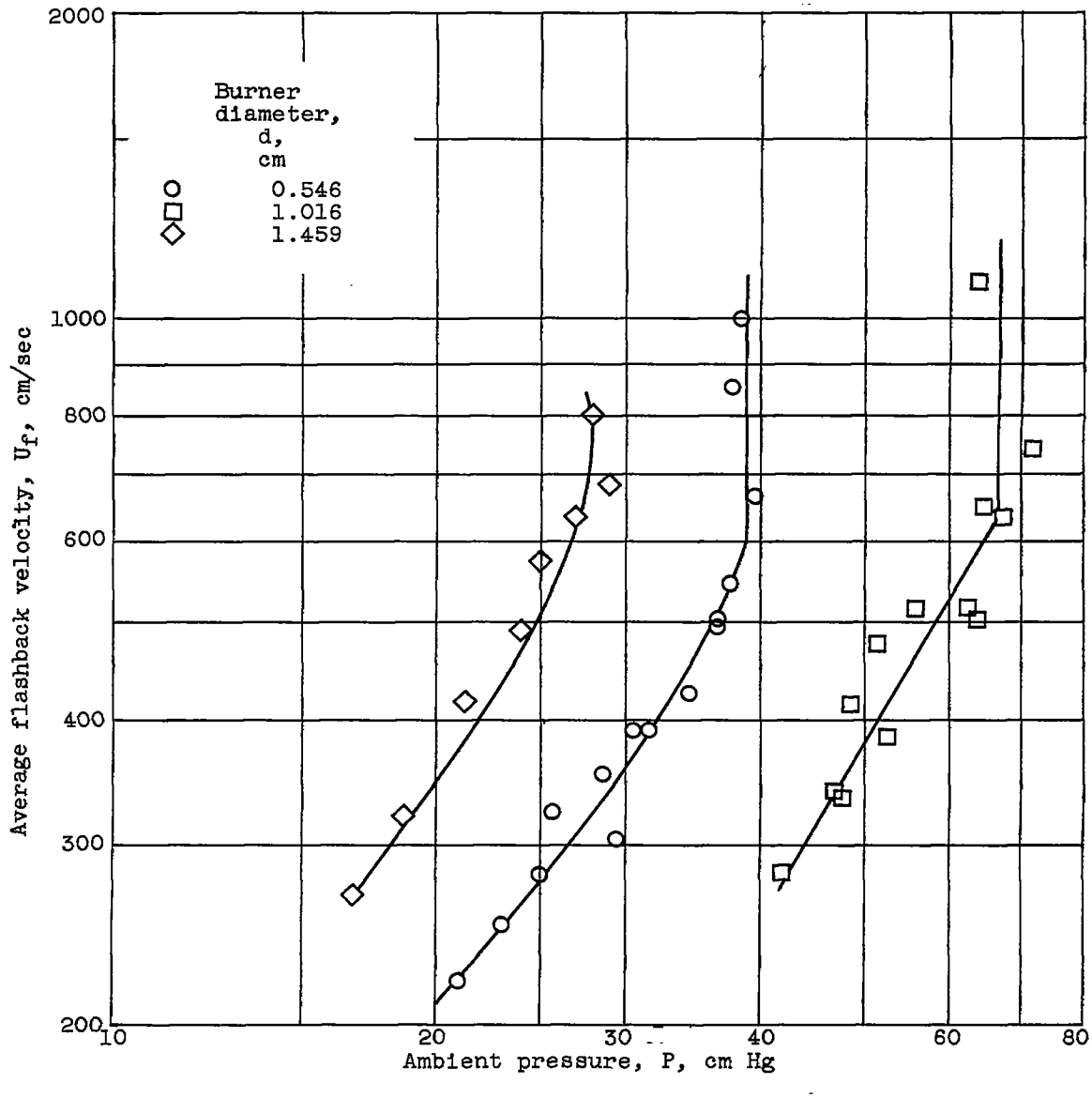

Figure 2. - Flashback velocity as function of ambient pressure. Equivalence ratio, 1.10; hydrogen, 31.5 percent.

4178

CI-3 back

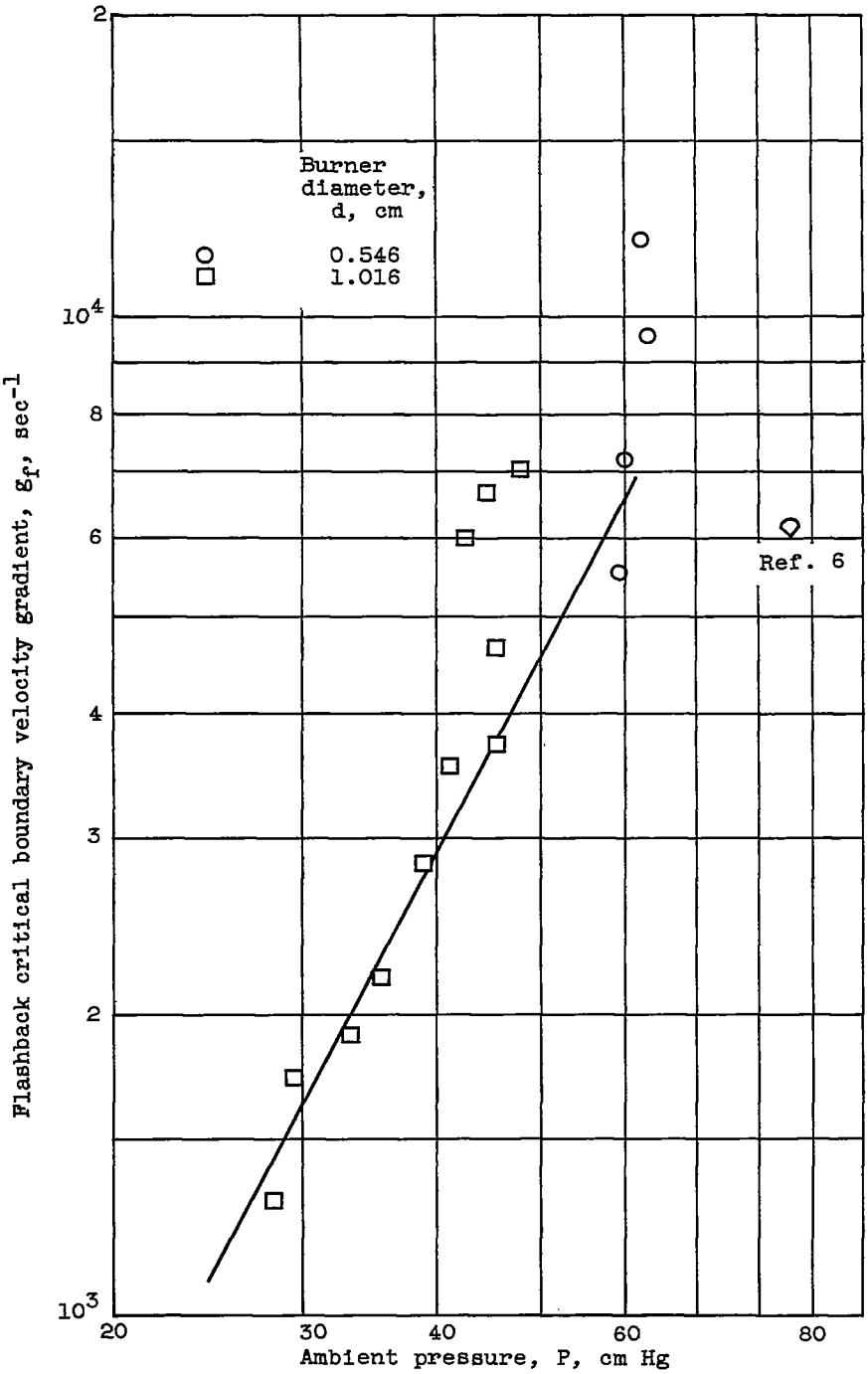

(a) Equivalence ratio, 0.80; hydrogen, 25 percent; pressure exponent for flashback, 1.99.

Figure 3. - Flashback velocity gradient as function of pressure at constant composition.

4178

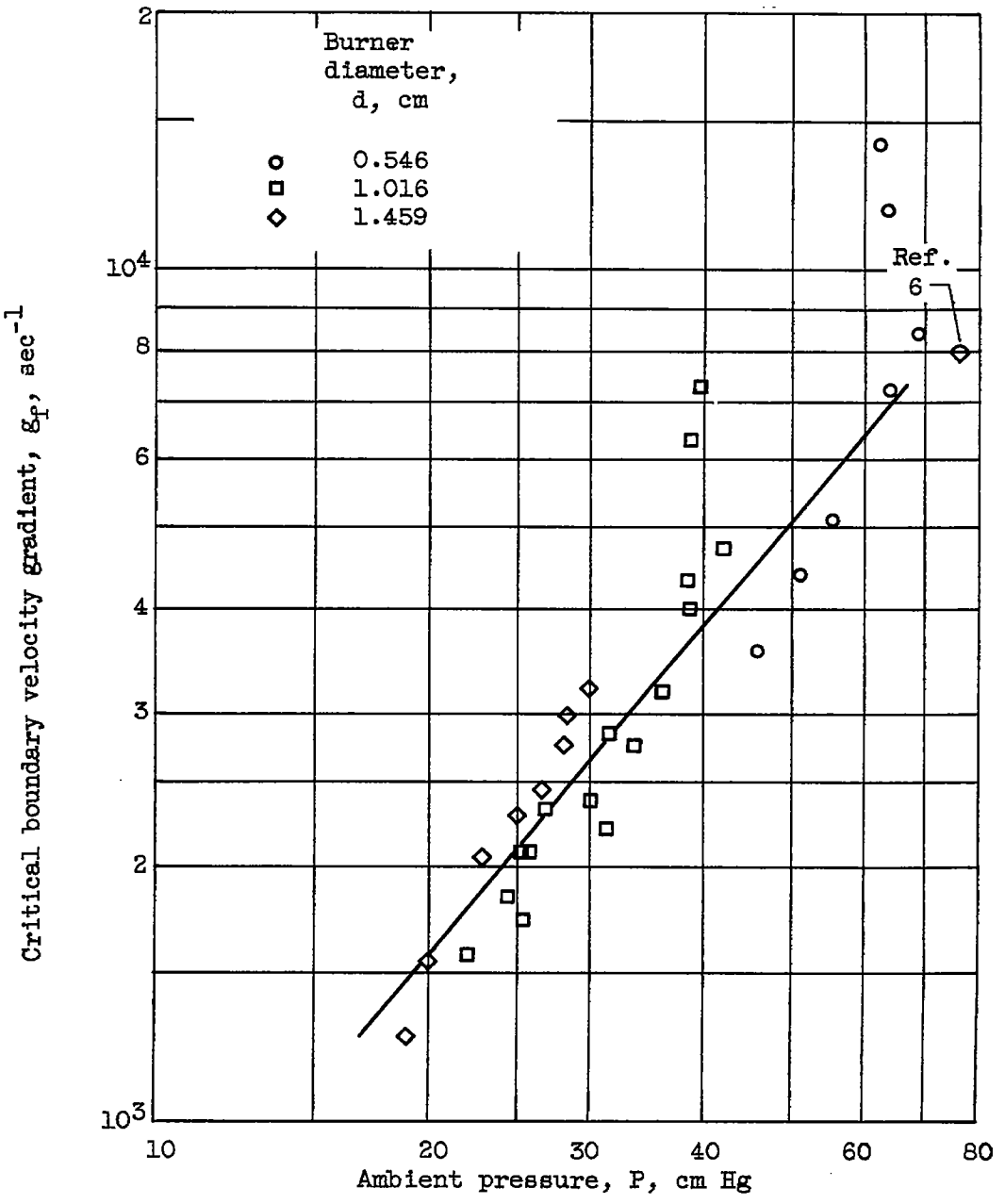

(b) Equivalence ratio, 0.95; hydrogen, 28.4 percent; pressure exponent for flashback, 1.27.

Figure 3. - Continued. Flashback velocity gradient as function of pressure at constant composition.

4178

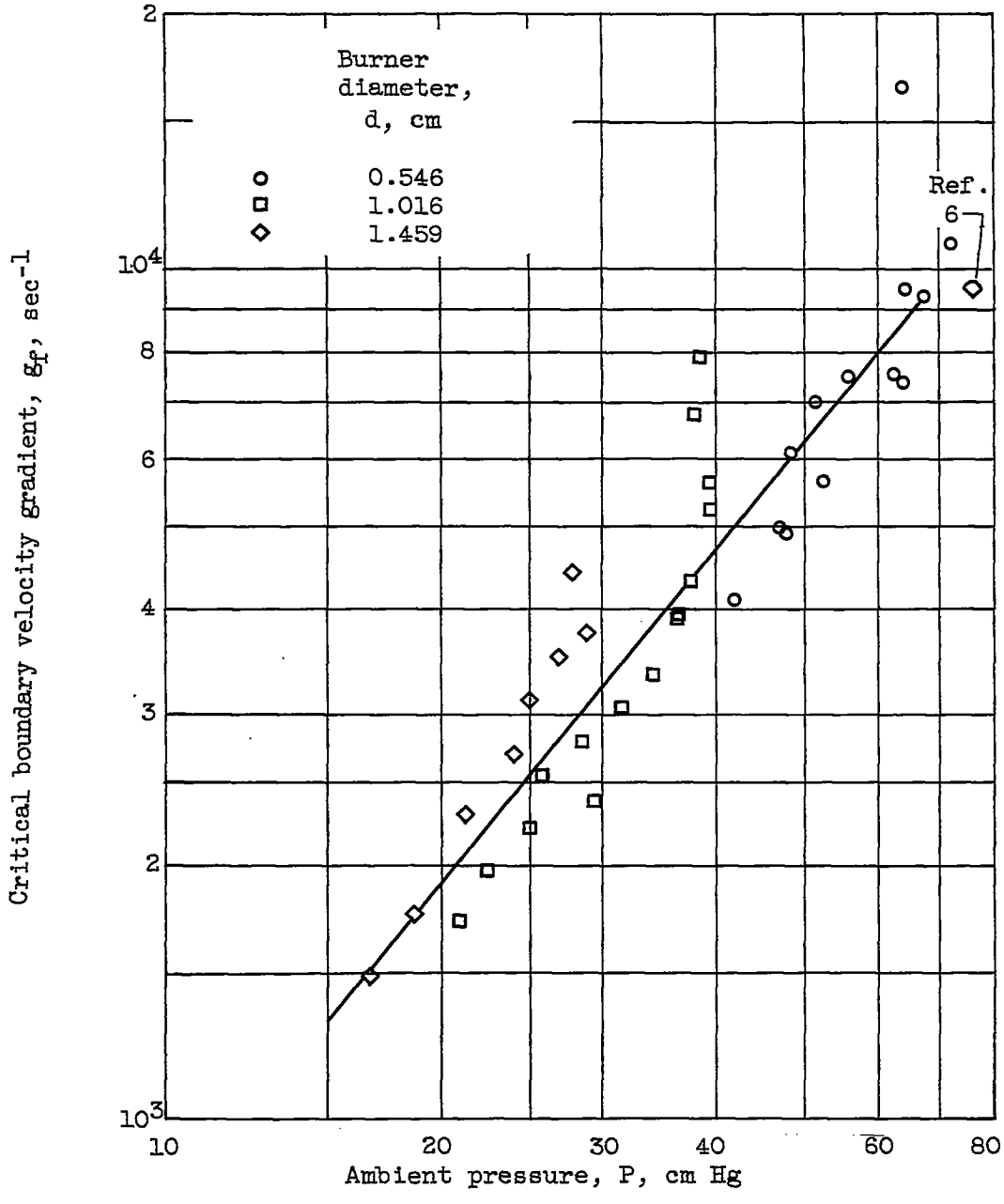

(c) Equivalence ratio, 1.10; hydrogen, 31.5 percent; pressure exponent for flashback, 1.28.

Figure 3. - Continued. Flashback velocity gradient as function of pressure at constant composition.

4178

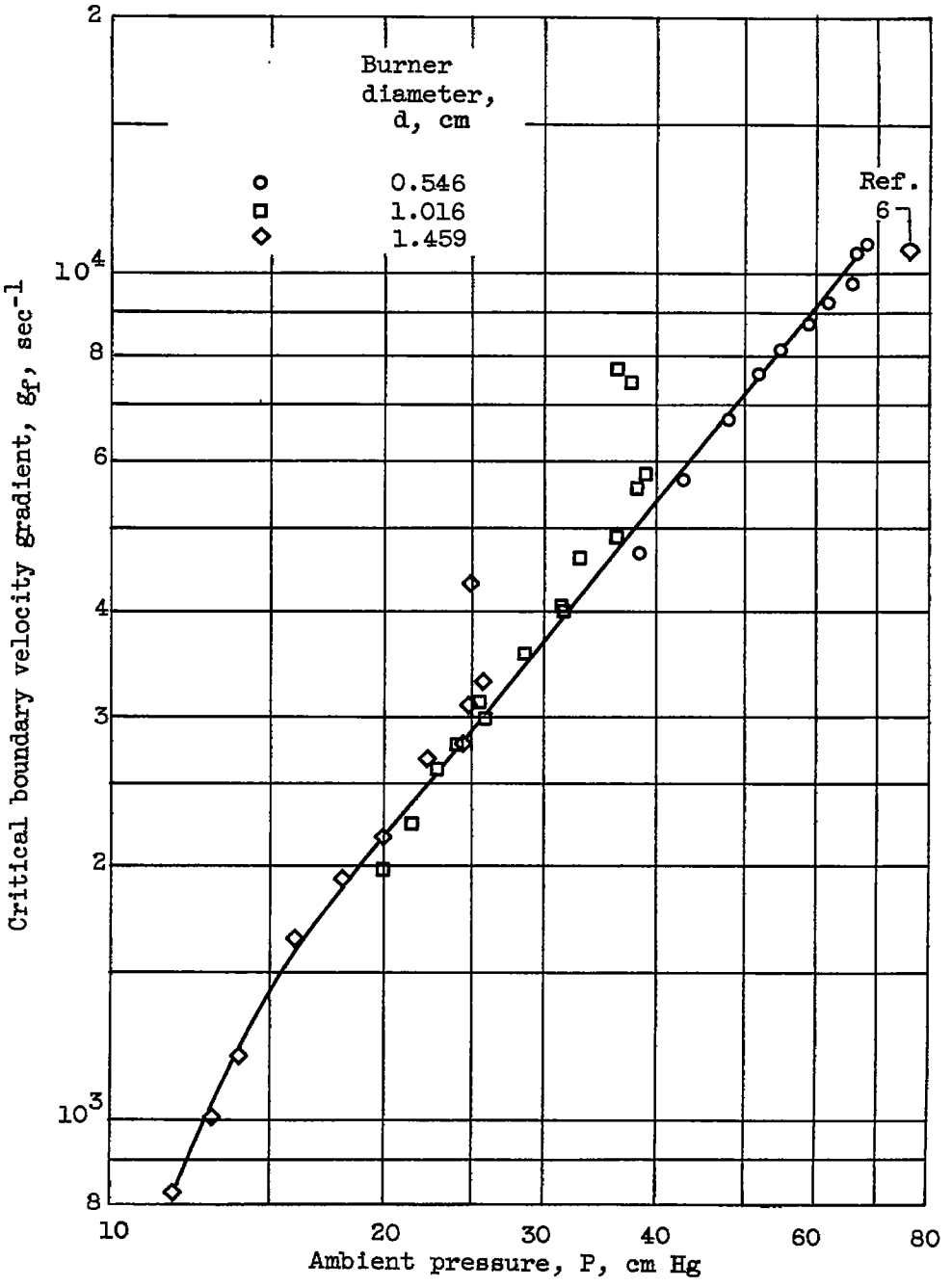

(d) Equivalence ratio, 1.30; hydrogen, 35 percent; pressure exponent for flashback, 1.35.

Figure 3. - Continued. Flashback velocity gradient as function of pressure at constant composition.

4178

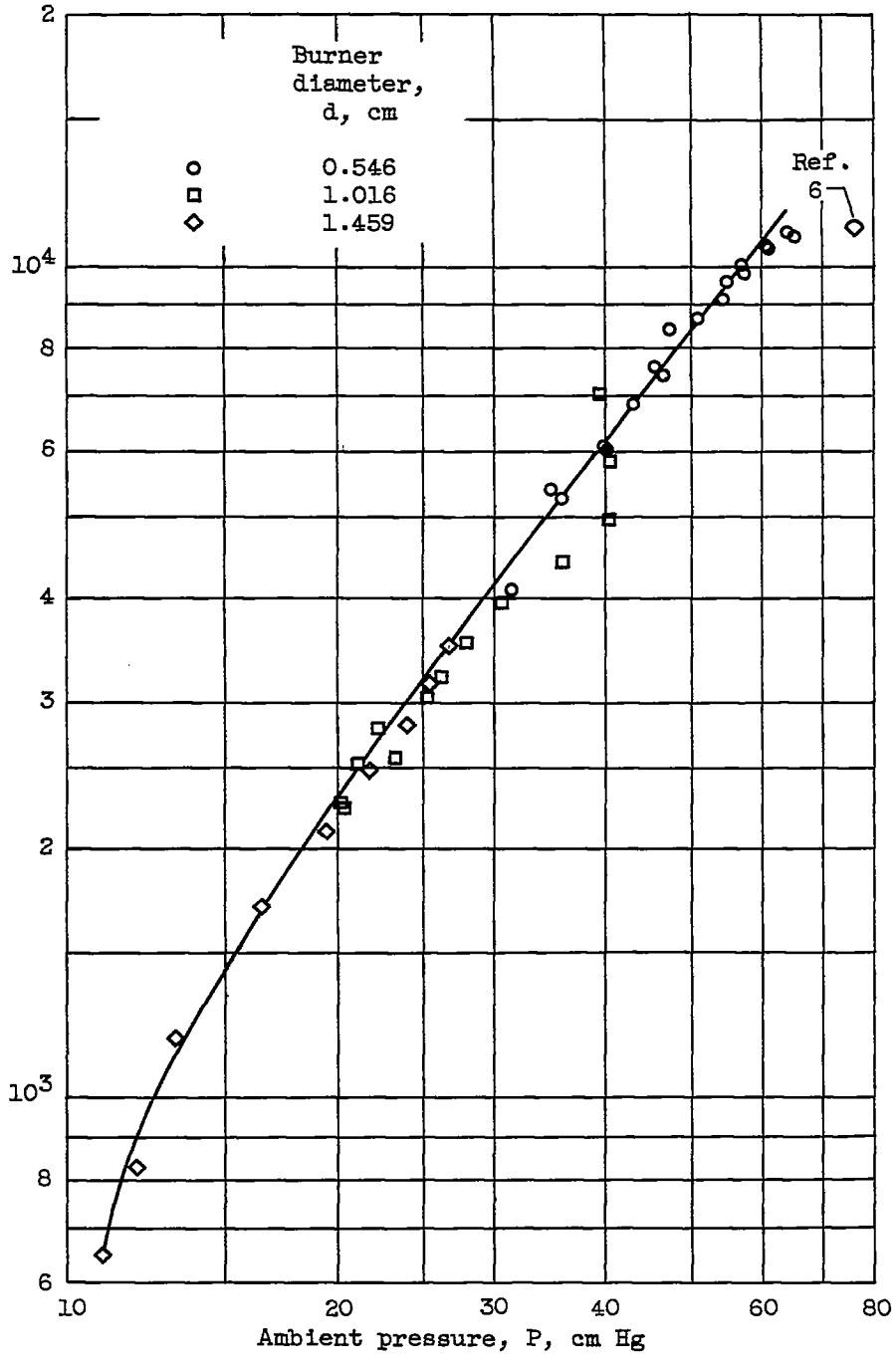

(e) Equivalence ratio, 1.50; hydrogen, 38.4 percent; pressure exponent for flashback, 1.42.

Figure 3. - Continued. Flashback velocity gradient as function of pressure at constant composition.

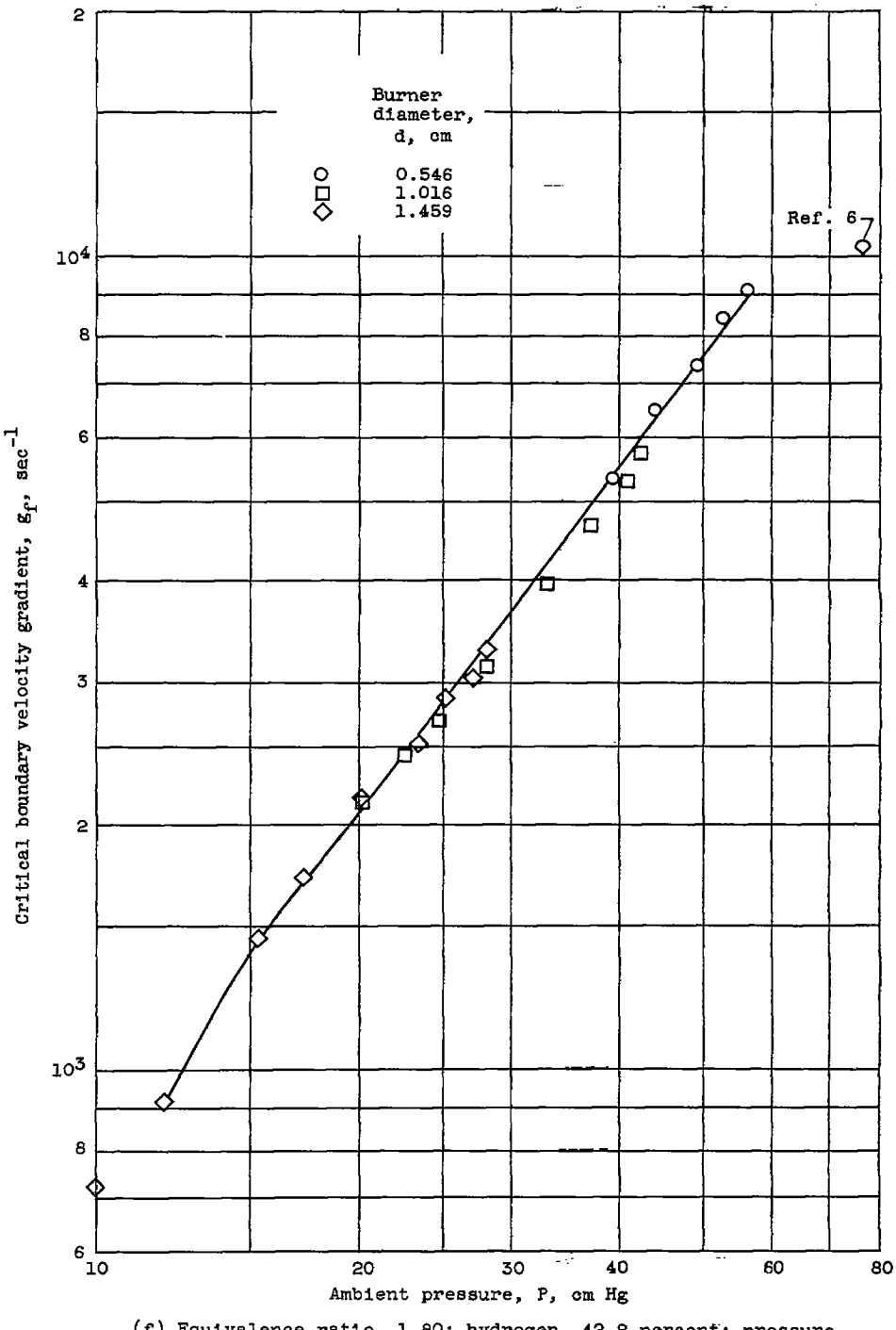

(f) Equivalence ratio, 1.80; hydrogen, 42.9 percent; pressure exponent for flashback, 1.40.

Figure 3. - Continued. Flashback velocity gradient as function of pressure at constant composition.

4178

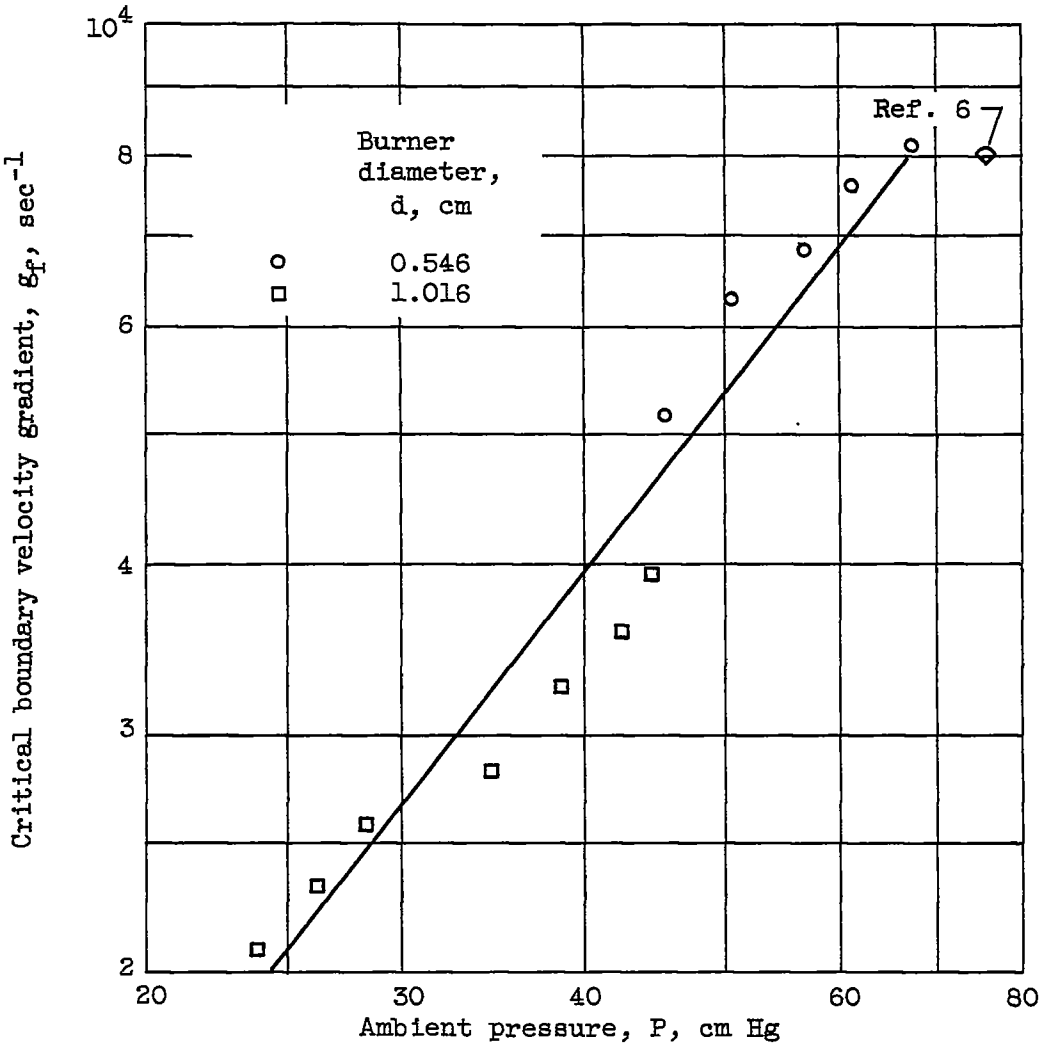

(g) Equivalence ratio, 2.25; hydrogen, 48.5 percent; pressure exponent for flashback, 1.35.

Figure 3. - Concluded. Flashback velocity gradient as function of pressure at constant composition.

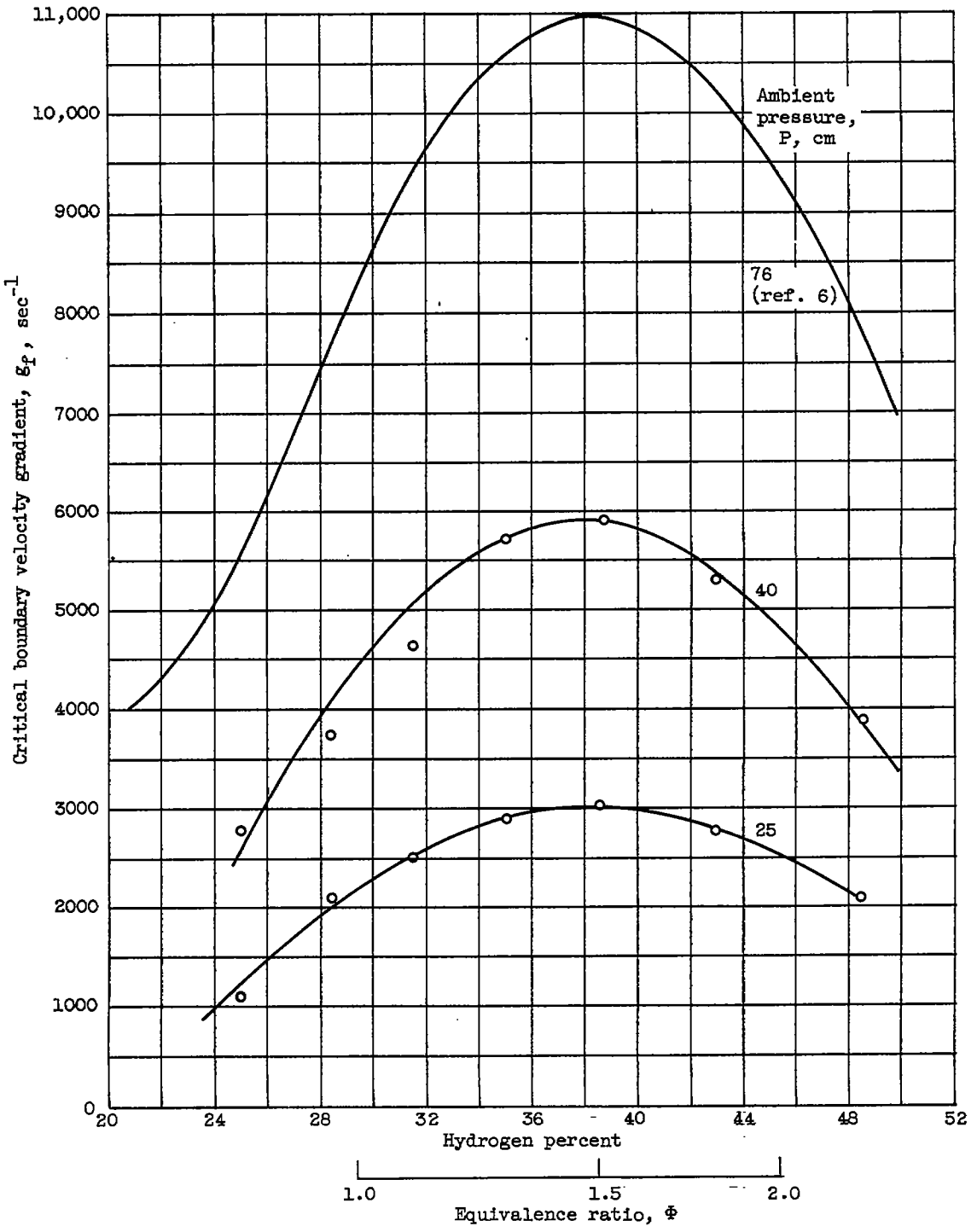

Figure 4. - Flashback velocity gradient as function of composition at constant pressure.

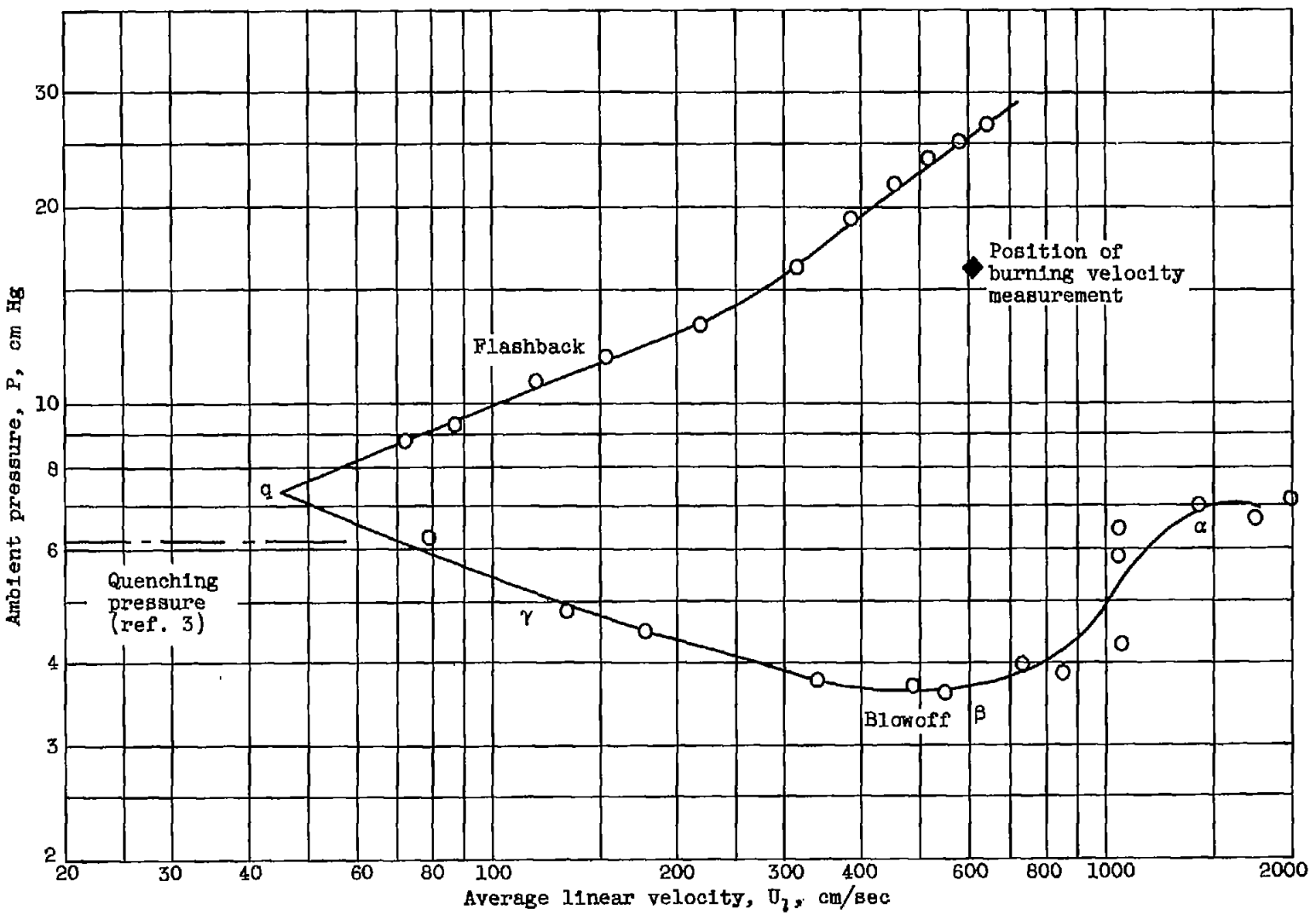

Figure 5. - Laminar stability loop for hydrogen-air system. Equivalence ratio, 1.50; burner diameter, 1.459 centimeters.

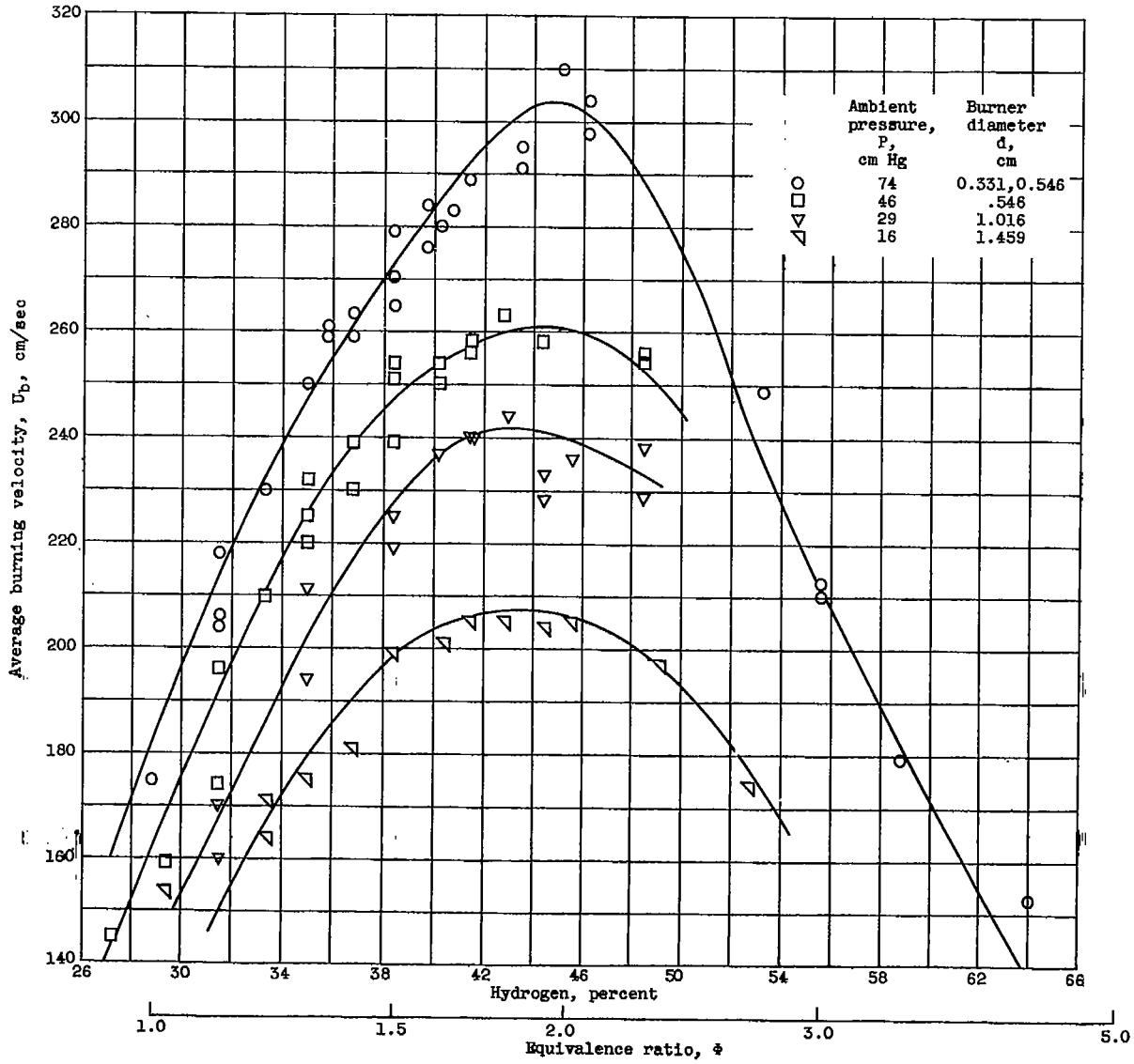

Figure 6. - Burning velocities of hydrogen-air flames.

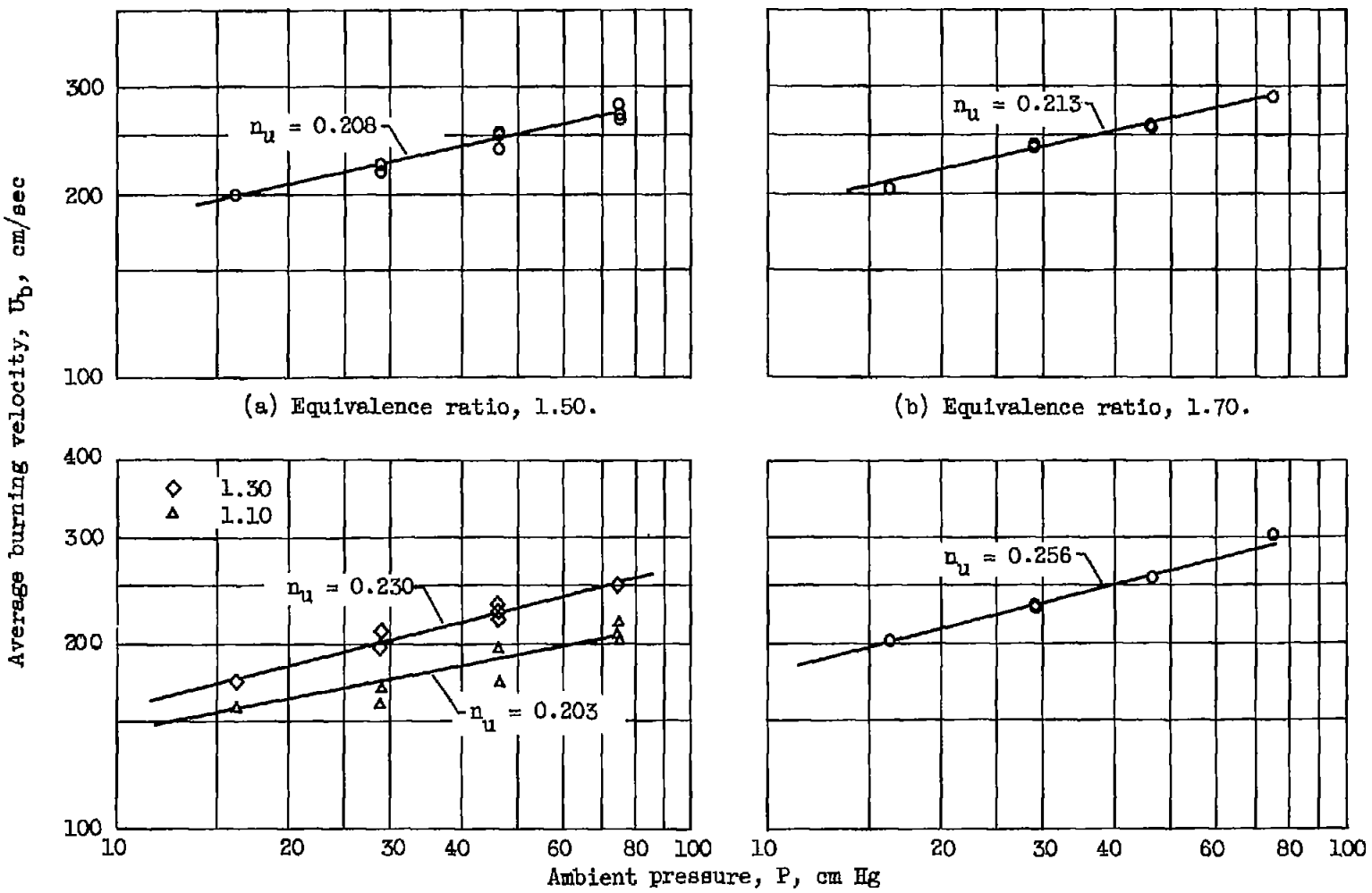

(a) Equivalence ratio, 1.50.

(b) Equivalence ratio, 1.70.

(c) Equivalence ratios, 1.30 and 1.10.

(d) Equivalence ratio, 1.90.

Figure 7. - Calculation of n_u ($U_b \propto P^{n_u}$).

NACA - Langley Field, Va.